Thermochimica Acta 499 (2010) 133–143

Contents lists available at ScienceDirect

Thermochimica Acta

journal homepage: www.elsevier.com/locate/tca

Post-mortem calorimetric and biochemical profiles of Chinook salmon (*Oncorhynchus tshawytscha*) white muscle following rested and exhausted harvesting

Leonard G. Forgan[a,*], Alistair R. Jerrett[a], Nicholas P.L. Tuckey[a], Malcolm E. Forster[b]

[a] New Zealand Institute for Plant and Food Research Limited, Box 5114, Port Nelson, Nelson 7043, New Zealand
[b] School of Biological Sciences, University of Canterbury, Private Bag 4800, Christchurch 8140, New Zealand

ARTICLE INFO

Article history:
Received 4 September 2009
Received in revised form 28 October 2009
Accepted 30 November 2009
Available online 3 December 2009

Keywords:
Anaerobic
Calorimetry
Energetics
Fish
Metabolism
Muscle

ABSTRACT

We report calorimetric and biochemical profiles of anoxic, post-mortem, white muscle from Chinook salmon subjected to rested and exhausted harvesting regimens. Heat output was greater ($P < 0.01$) in the rested group immediately after death (ca. 400 $\mu W g^{-1}$), and for the first 7 h post-mortem, reaching a nadir of about 15 $\mu W g^{-1}$ by 12 h. In exhausted animals, heat output was relatively unchanged at <10 $\mu W g^{-1}$ over 24 h. In both groups there was an exothermic event, occurring between 4 and 6 h post-mortem, amounting to a rise of ca. 35 $\mu W g^{-1}$. The greater heat production by the muscle from rested animals was accompanied by elevated pH (7.5 vs 6.7, $P < 0.05$), and higher concentrations of glycogen (16 vs 2 $\mu mol g^{-1}$), creatine phosphate (18 vs 0.1 $\mu mol g^{-1}$), ATP (6 vs 3.5 $\mu mol g^{-1}$) and potential energy (30 vs 7 $\mu mol g^{-1}$) than the exhausted group, which had elevated concentrations of lactate (43 vs 18 $\mu mol g^{-1}$, $P < 0.05$) and glucose (5 vs 2 $\mu mol g^{-1}$), over a number of hours post-mortem. The maintenance of potential energy in the form of ATP, glycogen and creatine phosphate for an extended period post-mortem indicates that tissue viability is extended in muscle from fish that are harvested in a rested manner.

1. Introduction

Seafood, primarily fish, constitutes about 20% of the animal protein consumed by humans worldwide [1]. The activity of the skeletal muscle of these animals at the time of harvest influences the energy charge of the tissue which can greatly affect the period of tissue viability before rigor mortis sets in and autolytic degradation begins [2–4]. White muscle in fish is typically recruited for "burst-type" predatory and escape behaviours [5–7] and possesses large carbohydrate stores which are utilised for anaerobic energy generation [8]. These stores of carbohydrate, as well as creatine phosphate and ATP are readily depleted by pre-mortem activity [9,10]. Thus it is desirable to use harvest regimens that conserve the energy generating potential in tissues. White muscle from fish that are rested harvested, frequently combining pre-harvest anaesthesia, invariably has a greater pH and extended pre-rigor period and shows improvements in a host of other indicators of meat quality (e.g. texture, colour, gaping, drip loss) relative to harvest procedures which exhaust animals [2,11–18]. These characteristics are highly desirable since they are associated with freshness and perceived quality of consumed items. To this end, the application of anaesthetics safe for human consumption in the aquaculture industry is being increasingly explored (e.g. [4,14,19–21]).

Extending viability in tissues is underpinned by knowledge of post-mortem metabolism and energetics, particularly energy stores and associated rates of depletion in the essentially anoxic conditions that accompany the loss of blood supply upon death. This understanding could help in the development of strategies to maximise harvest returns via handling protocols that slow the onset and progression of autolysis. The aim of the current study was to directly measure metabolic rate, using anoxic isothermal calorimetry, in post-mortem white muscle in a commercially harvested teleost species (Chinook salmon) subjected to two different harvest regimens. The first was a simulation of the exercise, crowding and netting procedures typical of some commercial aquaculture facilities (exhausted harvest). The second involved gradual anaesthesia with isoeugenol, involving the competitive blockade of neuromuscular transmission [22], before harvest with minimal "burst-type" activity and associated stress (rested harvest). These data are complimented by a parallel longitudinal study measuring the concentration of glycogen, glucose, lactate, creatine compounds, ATP and other important purine nucleotides,

* Corresponding author. Tel.: +64 3 539 1821; fax: +64 3 546 7049.
E-mail address: len.forgan@plantandfood.co.nz (L.G. Forgan).

0040-6031/$ – see front matter © 2009 Elsevier B.V. All rights reserved.
doi:10.1016/j.tca.2009.11.014

nucleosides and related bases in the muscle tissue. From these data, adenylate ratios to ATP, the total nucleotide pool, potential energy [23,24] and *K*-values [25] were calculated. Correlation analysis between heat output and the metabolites link changes observed in the two datasets. Both studies were performed within one degree of acclimation temperature (10 °C) to minimise the effect of temperature change on the post-mortem physiology.

2. Experimental

2.1. Animals

Female Chinook salmon (*Oncorhynchus tshawytscha*, Walbaum) (mass 1.898 ± 0.111 kg; fork length 51 ± 1 cm; condition factor (1.41 ± 0.04; $n = 28$, a measure of physical condition) were obtained from a local freshwater salmon farm (Isaac Salmon Farm, Canterbury, New Zealand) and transferred from commercial raceways, where they had been fed up until the time of transfer with Reliance Stock Feeds salmon pellets (CRT, Dunedin, New Zealand), into an 1800 l holding tank which had a continuous flow of high quality bore-water (a constant 11 °C). These fish were not fed and were left undisturbed for a minimum of 48 h. They were used within 1 week of transfer. All manipulations described in this manuscript were approved by the University of Canterbury Animal Ethics Committee.

2.2. Exhausted harvest

Individual fish were forced to swim in their holding tank for 5 min by chasing them with a large net. The fish was then manoeuvred into one quarter of the tanks volume using a wooden board, netted and placed into 20 l of water (11 °C) in an insulated transport container. The water was gassed with 100% oxygen for 10 min prior to transfer and the air-space in the container filled with oxygen before being transported to the University. Immediately on arrival (<25 min), the animals were restrained in a custom sling and killed by pithing the brain. Immediately after death, approximately 1 ml a 0.9% NaCl solution containing heparin sulphate (2500 IU ml^{-1} kg^{-1}) was injected into the dorsal aorta through the roof of the mouth, and allowed to circulate briefly before the animal was exsanguinated by cutting the ventral aorta, allowing it to bleed into the water for 2 min.

2.3. Rested harvest

Fish were anaesthetised to between stages 4–5 (not reactive to stimuli, but still showing limited ventilation [26] with AQUI-S™ (AQUI-S NZ, Lower Hutt, New Zealand) at a concentration of 22 ppm (0.012 g l^{-1} isoeugenol). Without alerting the animal, a concentrated stock solution of anaesthetic was gradually introduced into the holding tank gravimetrically and mixed with a Maxi-Jet MJ1000 water pump (Aquarium Systems, Loreggia, Italy). The animal was subsequently transported, killed and exsanguinated in the same way as the exhausted fish, except in this case the water used for transport contained 22 ppm AQUI-S™.

2.4. Muscle biopsy

Immediately after death, both fillets were removed from the carcass and skinned. A custom cylindrical stainless steel biopsy tool was then used to cut ca. 1 cm^3 cylindrical muscle plugs from the D1-block, 5 cm from the cephalad end of the fillet and stored in sterile glass vials filled with nitrogen. If necessary, the samples were trimmed to approximately 1 cm^3. The total preparation time from the time of death until the muscle biopsies were placed in the calorimeter did not exceed 10 min and all equipment was made sterile prior to use.

2.5. Calorimetry

Anaerobic heat output (μW) was measured in rested and exhausted white muscle tissue biopsies over a 24 h period at 10 °C (both $n = 8$). From each animal, three replicate white muscle biopsies were weighed and placed into sterile, pre-equilibrated, lidded Hasteloy® ampoules in a nitrogen filled bag and placed into one of 3 sample chambers, with a common reference ampoule containing 1 cm^3 distilled water, in a multi-cell differential scanning calorimeter (MC-DSC) (Calorimetry Sciences Corporation, South Provo, UT, USA) in isothermal (10 °C) mode. The heat output was recorded every 10 s over a 24 h period using Cpcalc software (Calorimetry Sciences Corporation) running on a desktop PC. The instrument took 20 min to equilibrate after the samples were inserted. These 20 min of data are not included in our analyses. The 10 min taken in the preparation of the biopsies has been added to the calorimetry equilibration time, resulting in a 30 min period from the time of death for which no heat output values are shown. The raw heat output from the samples was corrected by subtracting the background heat output of 1 cm^3 of distilled water at 10 °C. Values are expressed as wet mass per gram tissue.

2.6. Biochemical profile experiment

Removal of subsamples from the calorimeter whilst recording would have affected the temperature equilibration of the instrument and given erroneous readings. Therefore, a parallel experiment was conducted to accompany the calorimetry. In this longitudinal experiment, animals were harvested and muscle biopsies were prepared in exactly the same way as described for the two regimens above, except that four animals in each group were harvested together. An initial sample, representing time zero (equivalent to time zero in the calorimetry experiments), was rapidly freeze-clamped between two large aluminium blocks cooled in liquid nitrogen, then wrapped in aluminium foil and stored at −80 °C. A further ten samples, corresponding to 1, 2, 3, 4, 5, 6, 7, 8, 12 and 24 h post-mortem, were placed into 1.7 ml microtubes (Axygen, Union City, CA, USA) in a bag filled with nitrogen. Samples were stored in racks in an insulated temperature controlled box held at 10.0 ± 0.5 °C with a Tropicool XC3000A (Christchurch, New Zealand) temperature control unit with flow-through nitrogen. At the designated time the appropriate 4 samples were removed and frozen in the way described above. The temperature in the box was logged using a HOBO™ H8 Pro Series (Onset Computer Corporation, Bourne, MA, USA) temperature logger and BoxCar v3.6 software (Onset Computer Corporation, Bourne, MA, USA).

2.7. Cut surface tissue pH

Immediately after the muscle biopsies were removed, a transaxial cut was made through the two unused parts of the fillets. Using a Sensorex model 450C surface pH electrode (Garden Grove, CA, USA) with Radiometer model PHM84 pH meter (Copenhagen, Denmark) the initial cut surface pH of the white muscle was measured; mean of 6 measurements (a dorsal, medial and ventral measurement from each side of the fillet) from the freshly cut surfaces. At each subsequent time point during the experiment, an additional cut surface pH measurement was recorded from a freshly cut muscle biopsy; this time splitting the tissue biopsy with a scalpel blade and taking an average of the two cut surfaces.

2.8. Tissue extraction

2.8.1. Creatine compounds, purine nucleotides and nucleosides and related bases

The frozen muscle biopsies were ground in a porcelain pestle and mortar with liquid nitrogen. Approximately 100 mg of frozen powder was placed into a 1.8 ml Nunc cryotube (Roskilde, Denmark) vial with a pre-cooled spatula, 1.5 ml of ice cold 0.4N perchloric acid was added and the powder homogenised for ca. 1 min using a Heidolf Instruments DIAX 900 homogeniser on setting 6. The homogeniser blade was rinsed with 100 μl of perchloric acid and the mass made up to 1.80 g using perchloric acid. The extract was centrifuged at 6000 × *g* for 5 min and the supernatant transferred into a 1.7 ml microtube and neutralised (pH 7) with 2 M K_2CO_3. The extract was frozen at -80 °C until assayed (within 2 weeks).

2.8.2. Glucose, glycogen and lactate

Muscle samples were prepared in the same way as before except that the extraction medium was 500 μl of ice-cold 0.6N perchloric acid mixed in a ratio of 7:3 with absolute methanol and the mass was made up to 0.80 g. This homogenate was frozen at −80 °C until assayed (within 2 weeks). On thawing the extracts for analysis, a subsample was removed for the glycogen assay. This sample was neutralised with 2 M K_2CO_3. The remaining unneutralised homogenate was centrifuged at 10,000 × *g* for 5 min. The supernatant was neutralised in a new microtube using 2 M K_2CO_3 and further diluted with distilled water (1-fold). Glucose and lactate concentrations were determined in this extract.

2.9. Assays

All samples were measured in duplicate.

2.9.1. Glucose and glycogen assay

Glucosyl units were determined in the glucose and glycogen extracts using the method of Keppler and Decker [27], except that glucosyl units were measured in both extracts using the hexokinase method, employing a Roche Gluco-quant Glucose/HK assay kit (Mannheim, Germany) adapted for use in cuvettes. In this method the production of NADPH is stoichiometric with glucose conversion. The NADPH was quantified using a Shimadzu Corporation UV-1700 PharmaSpec spectrophotometer (Shimadzu Scientific Instruments, Columbia, USA) at 340 nm. Net glycogen-derived glucosyl units were determined by subtracting the tissue glucose concentration from the glycogen values.

2.9.2. Lactate assay

L-lactate in the neutralised and diluted muscle extracts was determined using the L-lactate dehydrogenase method, utilising a Megazyme L-lactic acid assay kit (Wicklow, Ireland). Here NADH production is stoichiometric with the dehydrogenation of L-lactate, which was measured as above.

2.9.3. Creatine compounds, purine nucleotides and nucleosides and related bases

Creatine compounds, purine nucleosides and nucleotides and related bases were separated by ion-pair reversed phase high performance liquid chromatography (HPLC) and quantified using UV–vis detection on a Shimadzu Scientific Instruments SIL-10A with a reversed phase 5 μm ODS (C18) 250 mm × 4.6 mm column protected with a C18 SecurityGuard guard column (both Phenomenex Inc., Torrance, CA, USA) based on the methods of Tuckey [28]. The neutralised muscle extracts were centrifuged at 10,000 × *g* and a 20 μl subsample injected onto the column. The column oven was held constant at 32 °C and sample cooler at 2 °C. A solvent gradient was run between two mobile phases over a 50 min period; mobile phase A (MPA) (0.05 M phosphate buffer (NaH_2PO_4) containing 2 g l^{-1} of HPLC grade tetrabutylammonium bisulfate (ion-pair reagent) (Fluka, ex Sigma–Aldrich Chemical Co.) (pH 5.5) and mobile phase B (MPB) (75% MPA and 25% acetonitrile, pH 5.5). System flow was maintained at 1 ml min^{-1} throughout the gradient cycle, which began with 100% MPA for 5 min followed by a 20 min gradient to 70% MPB. This was held for 3 min followed by a 2 min gradient back to 100% MPA. The column was then equilibrated with 100% MPA for a further 20 min. Dual wavelength UV–vis detection was used to accurately quantify the absorbance of both the creatine compounds (214 nm) and the other compounds (254 nm). Peak areas were calculated and adjusted with Shimadzu post-run software and compared to standards of known concentration.

2.10. Nucleotide ratios and total pool, K-values and potential energy

ATP:ADP, ATP:AMP and ATP:IMP ratios were calculated from the chromatography nucleotide data. The total nucleotide pool was calculated in μmol g^{-1} as the sum of ATP, ADP, AMP, IMP, NAD^+, inosine, hypoxanthine and uric acid. *K*-values were calculated using Eq. (1) [25].

$$K\text{-value}\,(\%) = \frac{\text{inosine} + \text{hypoxanthine}}{\text{ATP} + \text{ADP} + \text{AMP} + \text{IMP} + \text{inosine} + \text{hypoxanthine}} \times 100 \quad (1)$$

Potential energy was calculated using Eq. (2) [23,24].

$$\text{Pe}\,(\mu\text{mol g}^{-1}) = \text{creatine phosphate} + 2[\text{ATP}] + \text{ADP} \quad (2)$$

where Pe is the cell potential energy, phosphate bond state, or energetic state, since ATP has 2 and ADP and creatine phosphate have 1 available phosphate group for phosphorylation [23,24].

2.11. Chemicals

All chemicals were sourced from Sigma-Aldrich chemical company (St. Louis, MO, USA) unless otherwise stated.

2.12. Statistical analysis

All data were subjected to normality and equal variance testing prior to analyse. Differences within groups from the initial value (time zero, except for heat output where 1 h was used) for the calorimetric and biochemical profiles, pH, ratios (log 10), *K*-values and total nucleotide pool were determined by one-way repeated measures ANOVA followed by a Dunnett's post hoc test. Differences between the rested and exhausted treatments were determined using two-way repeated measures ANOVA and Bonferroni post hoc test, examining all comparisons. For comparison between the calorimetry data and the biochemical data, a smoothed value representing heat output at each h was used for analysis. Exhausted muscle calorimetry values were subtracted from the rested calorimetry values and the resulting net heat output was fitted with a single-phase exponential decay curve. Correlations between heat output and all of the metabolites and correlations between other relevant metabolites were calculated using Pearson r correlation analysis. All analysis was performed in Prism 4.00 (Graphpad software, San Diego, CA, USA). The significance level used was $P < 0.05$ but actual *P*-values or greater significance is shown where appropriate. All data appear as mean ± SEM, except the heat output data which appears as mean ± 95% CI.

3. Results

3.1. Harvest regimen associated activity

Animals subjected to the exhausted harvest protocol produced the "burst-type" swimming behaviour typical of salmonids (e.g. [5]). Fish displayed this behaviour for a variable amount of time, typically being unwilling to swim beyond about 4 min. The fish were relatively inactive when netted and handled after this treatment, although some fish continued to struggle. Animals subjected to the rested harvest regimen underwent anaesthesia without any "burst-type" swimming. While being netted and handled the fish remained immobile but ventilated steadily.

3.2. Calorimetry

The rested muscle produced a vastly different heat output profile than the exhausted muscle, which were different for the first 7 h post-mortem ($P < 0.001$). From an initial rate of ca. 400 $\mu W\,g^{-1}$, heat output from the rested group declined exponentially over a 12 h period to 15 $\mu W\,g^{-1}$, the rate dropping significantly after the first h of storage post-mortem ($P < 0.001$) (Fig. 1A). There was a clear exothermic event superimposed over the decline in heat output between 4 and 6 h. Muscle from exhausted animals had a very low initial heat output (<10 $\mu W\,g^{-1}$), rising ($P < 0.01$) to around 35 $\mu W\,g^{-1}$ at 5 and 6 h post-mortem before progressively decreasing again. This event mirrored the exothermic event in the rested muscle (Fig. 1A). The exothermic event and basal heat output present in both treatments was removed by subtracting the exhausted profile from the rested profile, resulting in a net heat output that was well described by a single-phase exponential decay model ($R^2 = 0.98$) (Fig. 1B). The predicted heat output from this model at time zero is 417 $\mu W\,g^{-1}$, reducing with a half time of 2.3 h.

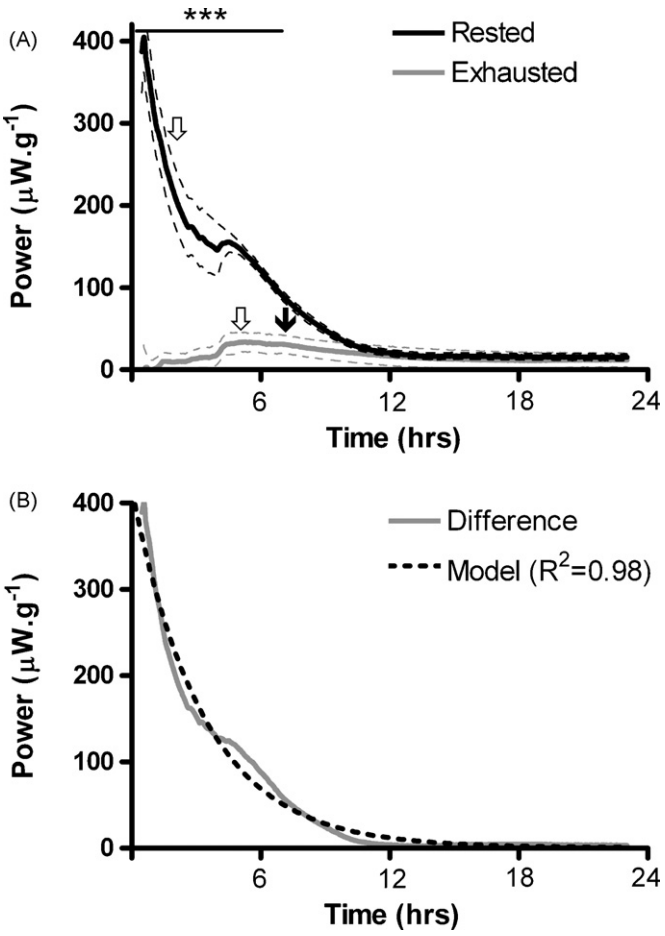

Fig. 1. Heat output of anoxic salmon white muscle at 10 °C over a 24-h period. (A) Rested (black line) and exhausted (grey line) heat output. Dashed lines are 95% CI. Asterisks (***) indicates significantly different between datasets ($P < 0.001$) (two-way repeated measures ANOVA with Bonferroni post hoc test). White arrows indicate the first significant change in heat output from initial (1 h) in the dataset. The black arrow indicates the first time at which heat output was no longer significantly different from initial. Both $n = 8$. (B) Difference between the rested and exhausted treatments (grey line) and a single-phase exponential decay model fitted to these data ($y = 417\exp(-8.366^{-5}x) + 0.5582$, half-time 2.3 h, $R^2 = 0.98$) (dashed black line).

3.3. Biochemical profiles

3.3.1. Glycogen, glucose, lactate and pH

The concentration of glycogen at the time of death in the rested group was 16 $\mu mol\,g^{-1}$, which declined significantly by the first-hour post-mortem to 7 $\mu mol\,g^{-1}$ ($P < 0.01$), reaching a value close to zero by 3 h (Fig. 2A). Exhausted muscles at time zero had <2 $\mu mol\,g^{-1}$ of glycogen, which declined by 2 h post-mortem to a value close to zero ($P < 0.01$). The rested and exhausted treatments were significantly different from each other at time zero and 1 and 2 h post-mortem ($P < 0.001$). The time zero muscle glucose concentration was elevated in exhausted animals at 5 $\mu mol\,g^{-1}$ versus 2 $\mu mol\,g^{-1}$ in the rested group ($P < 0.001$) (Fig. 2B). Glucose concentration in the rested group did not change from the initial value at any time point but the elevated concentration in the exhausted tissue had dropped from initial by 1 h post-mortem ($P < 0.05$). In both groups the concentration remained around 2–4 $\mu mol\,g^{-1}$ after this time. Lactate rose ($P < 0.01$) by 1 h in both groups from a time zero value of 18 and 43 $\mu mol\,g^{-1}$ to around 55 and 65 $\mu mol\,g^{-1}$ in rested and exhausted groups respectively (both $P < 0.01$) (Fig. 2C). Rested and exhausted treatments were different at time zero and 1, 2 and 4 h post-mortem ($P < 0.01$). Consistent with the rise in lactate, the pH fell to a nadir from 7.5 to 6.4 and from 6.7 to 6.0 by 3 h post-mortem in rested and exhausted groups respectively, the fall being significant by 1 h in both groups ($P < 0.01$). The pH of rested muscle was greater than that of exhausted muscle at time zero and at 1, 2 and 3 h post-mortem ($P < 0.05$).

3.3.2. Creatine phosphate, creatine, creatinine and potential energy

The time zero concentration of creatine phosphate in rested tissue was 18 $\mu mol\,g^{-1}$, which declined significantly ($P < 0.01$) by the first h of storage to just less than 5 $\mu mol\,g^{-1}$ and became undetectable by 12 h post-mortem (Fig. 3A). In contrast, the exhausted group concentration at time zero was 0.1 $\mu mol\,g^{-1}$, and was undetectable by 3 h post-mortem. The rested group concentration was higher at time zero and at 1 h of storage than in the exhausted muscle ($P < 0.01$). Potential energy decreased ($P < 0.01$) in rested and exhausted groups from an initial concentration of 30 to 9 $\mu mol\,g^{-1}$ and from 7 to 3 $\mu mol\,g^{-1}$ respectively by 1 h post-mortem (Fig. 3B). Rested tissue potential energy was greater than exhausted tissue at time zero, 1 and 2 h post-mortem ($P < 0.01$). There were no significant changes in the creatine concentration relative to time zero in either group, remaining around 70 $\mu mol\,g^{-1}$ (Fig. 3C). Furthermore, no difference between groups was detected at any time. Similarly, there were no significant changes in creatinine concentration relative to time zero in either group, remaining around 20 $\mu mol\,g^{-1}$ with no differences detected between groups (Fig. 3D).

3.3.3. ATP, ADP, AMP and NAD^+

In both groups the concentration of ATP, ADP and NAD^+ declined rapidly over the first 6 h post-mortem (Fig. 4). Initial ATP concentrations in rested and exhausted groups declined from 6 to 1.8 $\mu mol\,g^{-1}$ and from 3.2 to 0.9 $\mu mol\,g^{-1}$ respectively by 1 h post-mortem ($P < 0.01$). ATP concentration (Fig. 4A) was greater in the

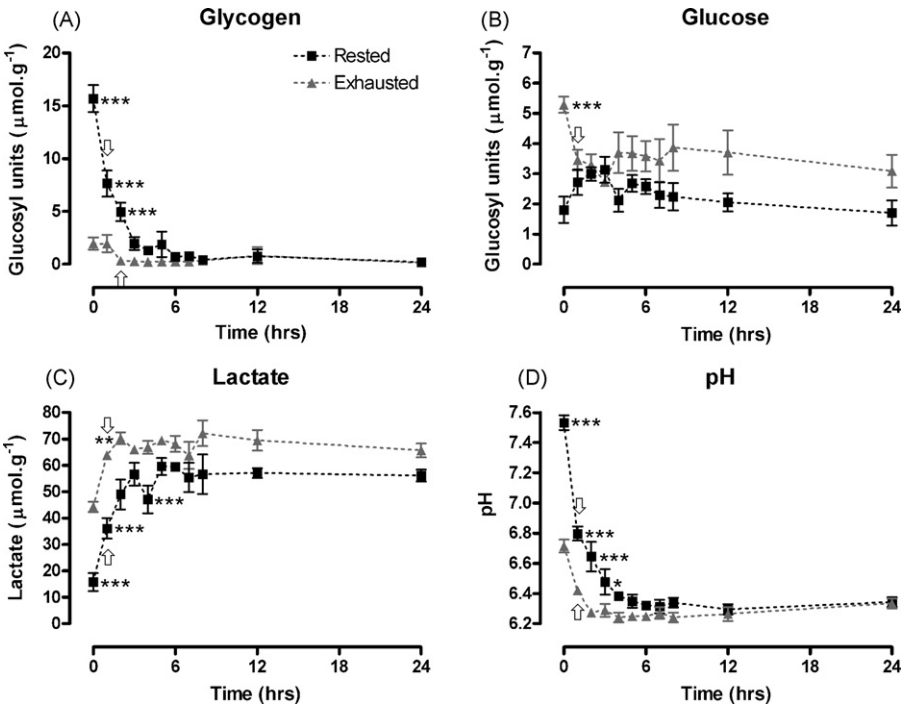

Fig. 2. Metabolite profiles from rested (black squares) and exhausted (grey triangles) anoxic white muscle at 10 °C over a 24-h period post-mortem. (A) Glycogen. (B) Glucose. (C) Lactate. (D) pH. $^{*}P < 0.05$, $^{**}P < 0.01$, $^{***}P < 0.001$ (two-way repeated measures ANOVA with Bonferroni post hoc test). White arrows indicate the first significant change in concentration from time zero of the dataset. Data are mean ± SEM. All $n = 4$.

rested group at 1 and 3 h post-mortem ($P < 0.05$). ADP concentration declined almost identically in both groups from around 1 μmol g^{-1} at time zero to around 0.4 μmol g^{-1} after 24 h (Fig. 4B). The concentration of ADP in the rested group was lower by 2 h and in the exhausted group by 3 h ($P < 0.01$). There were no significant differences in concentrations between the 2 groups at any time (Fig. 4B). AMP increased ($P < 0.01$) in concentration from 100 nmol g^{-1} to 300 nmol g^{-1} by 1 h post-mortem in the rested group, returning to the initial concentration by 7 h (Fig. 4C). In contrast, the exhausted group values were not different from the time zero concentration

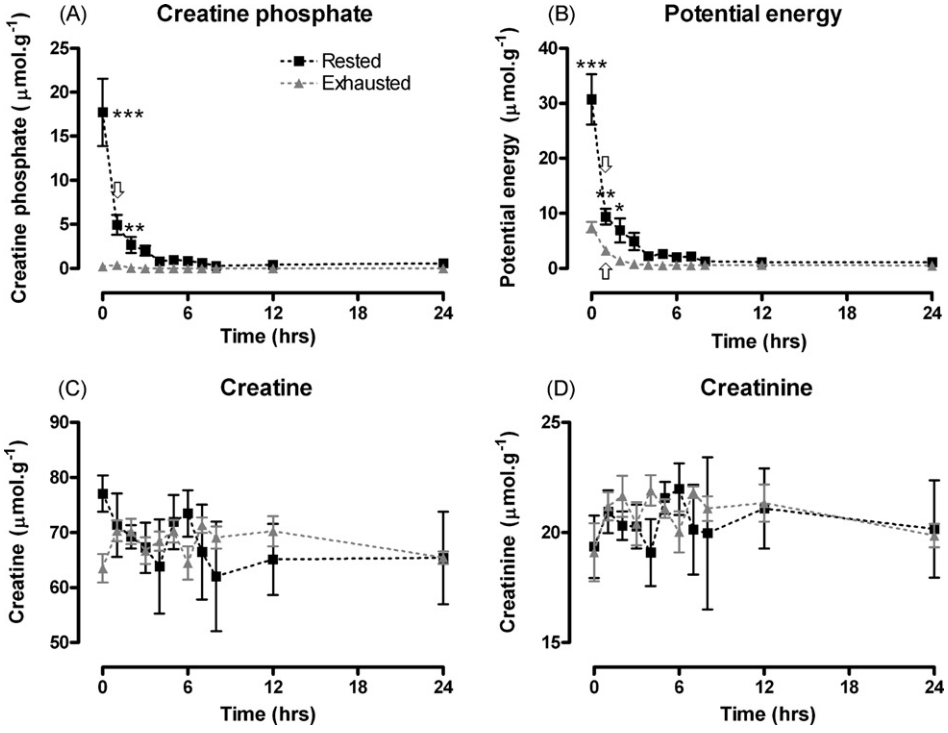

Fig. 3. Metabolite profiles from rested (black squares) and exhausted (grey triangles) anoxic white muscle at 10 °C over a 24 h period post-mortem. (A) Creatine phosphate. (B) Potential energy. (C) Creatine. (D) Creatinine. $^{*}P < 0.05$, $^{**}P < 0.01$, $^{***}P < 0.001$ (two-way repeated measures ANOVA with Bonferroni post hoc test). White arrows indicate the first significant change in concentration from time zero of the dataset. Data are mean ± SEM. All $n = 4$.

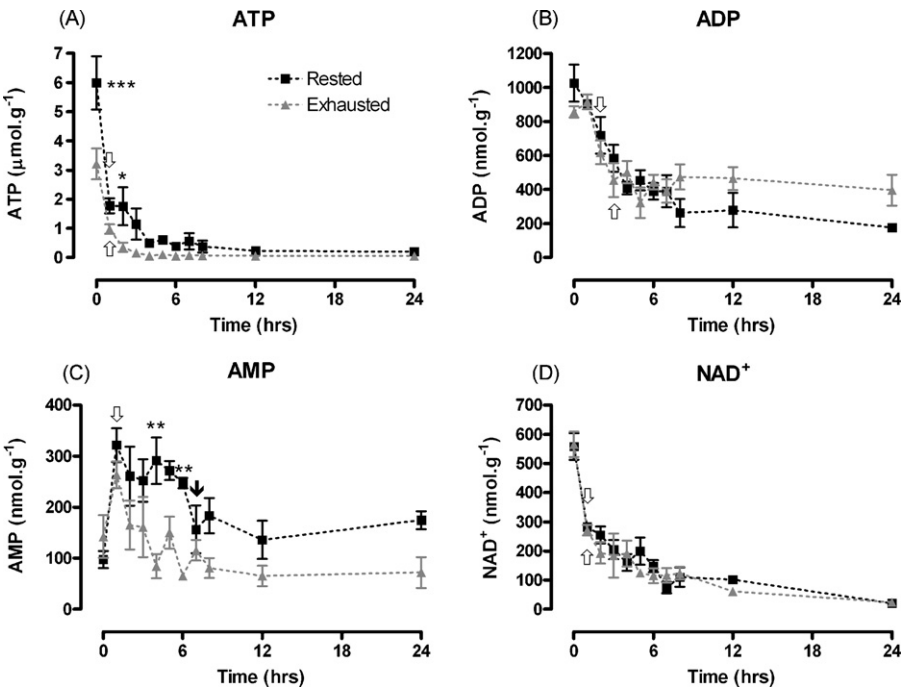

Fig. 4. Metabolite profiles from rested (black squares) and exhausted (grey triangles) anoxic white muscle at 10 °C over a 24 h period post-mortem. (A) ATP. (B) ADP. (C) AMP. (D) NAD^+. $^*P<0.05$, $^{**}P<0.01$, $^{***}P<0.001$ (two-way repeated measures ANOVA with Bonferroni post hoc test). White arrows indicate the first significant change in concentration from time zero of the dataset. Data are mean ± SEM. All $n=4$.

at any time point, remaining at around 100 nmol g^{-1}. The rested group had an elevated AMP concentration at 4 and 6 h post-mortem ($P<0.01$). In both groups, there was a significant decline in NAD^+ from an initial concentration of 550 nmol g^{-1} to 280 nmol g^{-1} by 1 h post-mortem ($P<0.01$), declining further to <50 nmol g^{-1} after 24 h (Fig. 4D). No difference in NAD^+ concentration was detected between groups at any time point.

3.3.4. IMP, inosine, hypoxanthine and uric acid

IMP concentration in the rested group rose ($P<0.01$) from just less than 2 μmol g^{-1} at time zero to 5.5 μmol g^{-1} at 1 h post-mortem, before gradually declining to initial concentrations by 12 h (Fig. 5A). IMP concentration in the exhausted group also increased ($P<0.01$) between time zero and 1 h, from 3.5 μmol g^{-1} to 6 μmol g^{-1}, before declining to initial concentrations by 24 h.

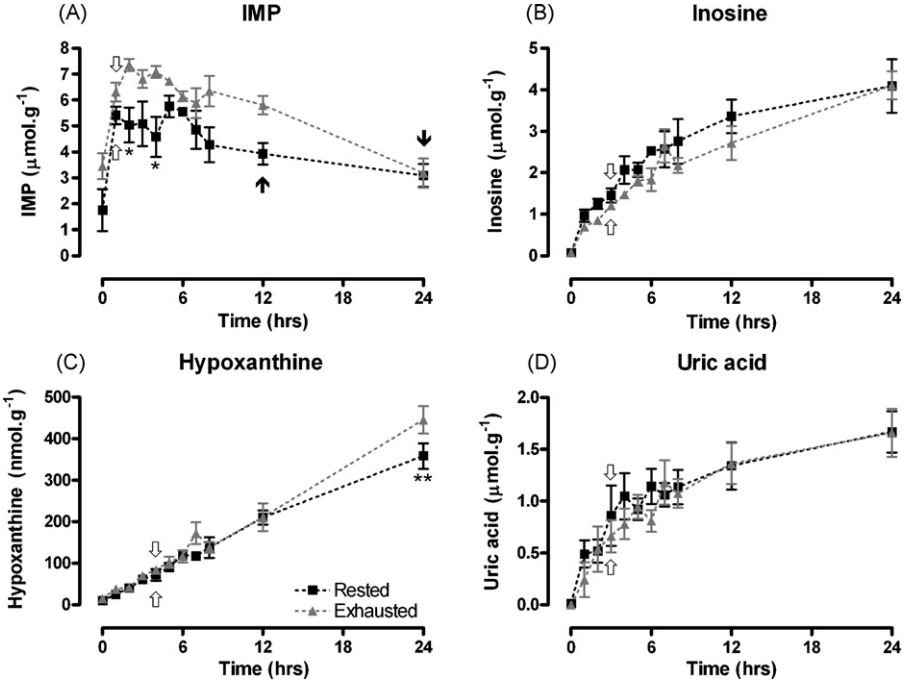

Fig. 5. Metabolite profiles from rested (black squares) and exhausted (grey triangles) anoxic white muscle at 10 °C over a 24 h period post-mortem. (A) IMP. (B) Inosine. (C) Hypoxanthine. (D) Uric acid. $^*P<0.05$, $^{**}P<0.01$, $^{***}P<0.001$ (two-way repeated measures ANOVA with Bonferroni post hoc test). White arrows indicate the first significant change in concentration from time zero of the dataset. Black arrows indicate the first time at which the concentration was no longer significantly different from the initial. Data are mean ± SEM. All $n=4$.

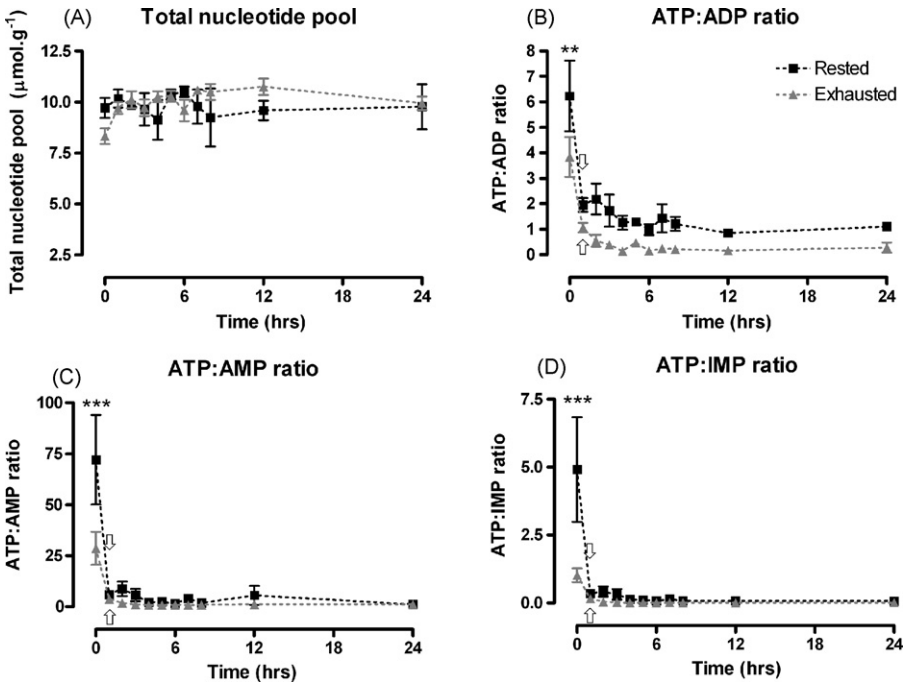

Fig. 6. Ratios between selected metabolites and the total nucleotide pool from rested (black squares) and exhausted (grey triangles) anoxic salmon white muscle at 10 °C over a 24 h period post-mortem. (A) Total nucleotide pool. (B) ATP:AMP. (C) ATP:IMP. (D) ATP:ADP. $^{*}P<0.05$, $^{**}P<0.01$, $^{***}P<0.001$ (two-way repeated measures ANOVA with Bonferroni post hoc test on the log 10 of ratios). White arrows indicate the first significant change in concentration from time zero of the dataset. Data are mean ± SEM. All $n=4$.

IMP concentration was significant higher ($P<0.05$) in rested tissue at 2 and 4 h post-mortem. Inosine was undetectable at time zero, but had increased in concentration above initial by 3 h post-mortem in both groups ($P<0.01$), further increasing to values around 4 μmol g^{-1} by 24 h (Fig. 5B). There was no difference detected between treatments at any time. Hypoxanthine was also undetectable at time zero in both the rested and exhausted groups (Fig. 5C), the concentration gradually increasing and becoming elevated by 4 h post-mortem ($P<0.01$). By 24 h the exhausted group had accumulated ($P<0.01$) more hypoxanthine than the rested group, at 450 nmol g^{-1} versus 350 nmol g^{-1} respectively. Uric acid concentration changed in a similar manner to inosine and hypoxanthine, increasing ($P<0.01$) from undetectable concentrations at time zero to 500 nmol g^{-1} by 3 h, further increasing to 1.5 μmol g^{-1} by 24 h in both groups (Fig. 5D).

3.3.5. Nucleotide ratios and total pool, K-values and correlations

The total nucleotide pool in both the rested and exhausted groups remained at a constant concentration of around 10 μM over the 24 h period post-mortem, with no difference determined between treatments at any time (Fig. 6A). For both treatments the ratios of ATP to ADP, AMP and IMP all showed a significant decline ($P<0.01$) by the first h post-mortem (Fig. 6B–D). At time zero all three ratios were lower (all $P<0.01$) in the exhausted group.

The *K*-values in both groups rose from an initial value of 0% to a peak of around 55% by 24 h, becoming greater ($P<0.01$) than the initial at 2 and 3 h post-mortem in the rested and exhausted groups respectively. *K*-values in the exhausted treatment were lower ($P<0.05$) than in the rested group at 12 h post-mortem.

Correlations between metabolites and heat output from 1 h onwards are summarised in Table 1. The only parameters that

Table 1
Summary of correlation analysis between metabolic heat output and metabolite concentrations, *K*-values, total nucleotide pool and potential energy in rested and exhausted anoxic salmon white muscle at 10 °C from 1 to 24 h. $^{*}P<0.05$, $^{**}P<0.01$, $^{***}P<0.001$ and ns is not significant. The Pearson r coefficient ranges from −1 to +1, corresponding to a perfect negative and positive correlation respectively; $n=4$.

Correlate	Rested				Exhausted			
	Pearson r	*P*-value	Summary	r^2	Pearson r	*P*-value	Summary	r^2
Glycogen	0.91	0.0002	**	0.84	0.45	0.1884	ns	0.21
Glucose	0.73	0.0170	*	0.53	−0.61	0.0587	ns	0.38
Lactate	−0.76	0.0110	*	0.56	0.31	0.3790	ns	0.09
pH	0.89	0.0005	**	0.80	−0.76	0.0100	*	0.58
ATP	0.89	0.0004	**	0.80	−0.69	0.0253	*	0.49
Creatine phosphate	0.91	0.0002	**	0.83	−0.66	0.0300	*	0.44
Creatine	0.55	0.0960	ns	0.31	−0.06	0.8700	ns	<0.01
Creatinine	0.10	0.7910	ns	<0.01	−0.01	0.9880	ns	<0.01
ADP	0.97	<0.0001	***	0.94	−0.76	0.0110	*	0.56
AMP	0.87	0.0011	**	0.76	−0.55	0.0940	ns	0.31
NAD^+	0.92	0.0001	***	0.86	−0.44	0.2020	ns	0.19
Hypoxanthine	−0.82	0.0037	**	0.67	0.03	0.9288	ns	<0.01
Inosine	−0.93	<0.0001	***	0.87	0.27	0.4600	ns	0.07
Uric acid	−0.92	0.0001	***	0.85	0.35	0.3190	ns	0.12
IMP	0.71	0.0217	*	0.50	0.09	0.8050	ns	0.01
Total nucleotide pool	0.33	0.3449	ns	0.11	0.33	0.3510	ns	0.11
K-values	−0.93	0.0001	***	0.86	0.19	0.5800	ns	0.04
Potential energy	0.93	<0.0001	***	0.86	−0.71	0.0209	*	0.51

Table 2
Summary of correlation analysis between selected metabolites in rested and exhausted anoxic salmon white muscle at 10 °C over 24 h. $^{*}P<0.05$, $^{**}P<0.01$, $^{***}P<0.001$ and ns is not significant; $n=4$.

Correlate	Rested				Exhausted			
	Pearson r	*P*-value	Summary	r^2	Pearson r	*P*-value	Summary	r^2
Glycogen vs pH	0.99	<0.0001	***	0.99	0.82	0.0010	**	0.68
Glycogen vs lactate	−0.96	<0.0001	***	0.92	−0.69	0.0170	*	0.48
Glycogen vs ATP	0.98	<0.0001	***	0.95	0.82	0.0020	**	0.67
Lactate vs pH	−0.96	<0.0001	***	0.92	−0.095	<0.0001	***	0.9
ATP vs pH	0.99	<0.0001	***	0.96	0.098	<0.0001	***	0.96
ATP vs creatine phosphate	0.99	<0.0001	***	0.98	0.66	0.0300	*	0.43
ATP vs ADP	0.85	0.0011	*	0.71	0.76	0.0060	*	0.58
ATP vs AMP	−0.35	0.3010	ns	0.12	0.35	0.2890	ns	0.124
ATP vs NAD	0.95	<0.0001	***	0.90	0.095	<0.0001	***	0.89
ATP vs IMP	−0.61	0.0480	*	0.37	−0.52	0.0960	ns	0.28

did not significantly correlate ($P>0.05$) with heat output in the rested group were creatine, creatinine and the total nucleotide pool. In contrast, only pH, ATP, creatine phosphate and potential energy were significantly correlated ($P<0.05$) with heat output in the exhausted muscles, and in these the correlations were all negative. A second series of correlation analyses is presented in Table 2, which includes time zero. In these correlations, declines in glycogen were correlated ($P<0.0001$) with falling pH, lactate and ATP in both groups. Conversely, there is an inverse correlation between lactate and pH in both groups. In both groups the decline in ATP concentration was correlated ($P<0.0001$) with a fall in pH, creatine phosphate, ADP and NAD^+. Changes in ATP and IMP were inversely correlated ($P<0.05$) in rested but not exhausted animals, while changes in ATP and AMP were not correlated in either group.

4. Discussion

The heat output and metabolite concentrations in the muscles of anaesthetised animals of the rested group contrasted starkly with those in the exhausted group. An initial heat output of approximately 400 $\mu W\,g^{-1}$ in the rested group declined exponentially over 12 h (Fig. 1A). Conversely, the exhausted group exhibited a low (<10 $\mu W\,g^{-1}$) and relatively unchanging heat output. This difference in heat output suggests that in the white muscle of animals that were rested harvested there was a period of extended tissue viability post-mortem, relative to the exhausted animals. In the rested group, heat output positively correlated with changes in the concentration of glucose, glycogen, pH, ATP, ADP, AMP, IMP and NAD^+ as well as the derived parameter, potential energy (a proxy of ATP turnover [23,24]) (Table 1). As might be expected, the concentration of lactate, inosine, hypoxanthine and uric acid, as well as the *K*-values showed a negative correlation with heat output in the rested group. These data suggest that the concentrations of key metabolites such as ATP, ADP, creatine phosphate and stores of glycogen (Figs. 2A, 3A, 4A and B), which are elevated in the rested group, contribute to the total heat output. Thus, the decline in heat output represents a loss of energy stores.

Despite the elevated metabolic rate reported here, it is clear that from the time of death, both groups have begun losing high energy compounds as the myocytes become unable to regenerate metabolites and redox potential, presumably leading to autolysis. In viable cells, ATP, ADP, NAD^+ and creatine phosphate do not fluctuate greatly in concentration, despite large changes in ATP turnover [29]. For example, in a study using a perfused dog gastrocnemius preparation, creatine phosphate, inorganic phosphate and ATP concentrations showed no measurable changes in concentration despite an 18-fold change in the rate of ATP turnover [30]. This phenomenon is known as the stability paradigm [31] and is thought to be facilitated by the three-dimensional intracellular structure within cells that constrains metabolite behaviour, and can increase the rates of reactions dramatically [32]. Nevertheless, measurable changes in the concentrations of ATP, creatine phosphate and glycogen have been induced by pre-mortem activity in fish [8,9,10,33–37]. Furthermore, during anoxia, van den Thillart et al. [38] demonstrated that after creatine phosphate stores were exhausted by 85%, ATP fell and IMP accumulated in crucian carp (*Carassius carassius*) and goldfish (*Carassius auratus*) muscle. Thus high energy demand and environmental/metabolic hypoxia in fish muscle *in vivo* is associated with a decline in tissue ATP and other metabolite concentrations.

In the current study, ATP fell rapidly in both groups concurrent with a drop in glycogen and creatine phosphate (Figs. 2A, 3A and 4A). Thus ATP concentration was dependent on the concentration of these two metabolites. There is no evidence from our data that creatine phosphate, via the creatine kinase pathway, or anaerobic glycolysis maintained ATP concentration. Of note is the very low concentration of creatine phosphate and glycogen in the exhausted group, which indicates that much of the capacity to provide rapid ADP phosphorylation had been compromised by pre-mortem activity. Consequently ATP concentration fell more rapidly. The similar falls in the ATP:ADP, ATP:AMP and ATP:IMP ratios reflects in most part the rapid fall in ATP concentration in both treatments (Fig. 6B–D). The ATP:ADP ratio is consistently lower in the exhausted group, reflecting the lower ATP concentrations in exhausted muscle over the course of the experiment. Differences in the ATP:AMP and ATP:IMP ratio are diminished by 1 h post-mortem in both treatments due to the fall in ATP but also the pronounced rise in AMP and IMP post-mortem, which is suggestive of depleted ATP stores and impaired ATP supply. The potential contributions of intracellular lipid and protein to ATP generation in our study are unknown, but certainly failed to bolster ATP concentrations. Lipid is favoured for oxidation during sustained aerobic locomotion [39,40] and in aerobic recovery from exhaustive exercise [41], which would have been impossible under the anoxic conditions of our study. Similarly, protein oxidation could not have contributed to ATP generation.

Interestingly, there is a clear exothermic event in the heat output profiles of both groups between 4 and 6 h. The timing of this event suggests that it is not directly associated with energy metabolism. Instead it is likely to be associated in some way with the loss of cell viability following death. If the event was associated with energy metabolism, we would have expected it to have registered earlier in the exhausted group, in which ATP and creatine phosphate concentrations fell to minimal values between 1 and 3 h, well before the rested muscle. Further to this, there are no changes in metabolite concentrations in these tissues that correlate with the exothermic event. It is unlikely that an event associated with energy metabolism, resulting in increased heat output, would coincide with almost completely depleted energy stores.

Instead, a variety of autolytic processes might be responsible for the exothermic event. For example, the folding and unfolding of proteins involves enthalpy changes [42]. Conformational changes can be influenced by the hydrogen ion concentration, but this can be ruled out as the pH fell much more rapidly in the exhausted group (Fig. 2D). Of note is that ADP and NAD^+ plateaued at 4 h in both rested and exhausted muscle (Fig. 4B and D); ADP was reduced to one third and NAD^+ reduced to one sixth the concentration at 1 h post-mortem. Perhaps the concentrations of ADP and NAD^+ at this time critically restricted the production of ATP through substrate and reducing capacity limitations respectively. It is possible that bacterial proliferation contributed to the exothermic event/s. However, the chances of a bacterial contribution were low for several reasons; the biopsies were prepared using sterile instruments, the ampoules were sterilised and the samples were kept in a nitrogen atmosphere during the course of the experiment, which would preclude the proliferation of aerobic bacteria. In addition, the appearance at 4 h and disappearance at 6 h of the exothermic event is not consistent with the exponential growth typical of bacteria.

To eliminate the effects of the exothermic event/s on metabolic rundown, the exhausted data was subtracted from the rested data at corresponding time points (Fig. 1B). The single-phase exponential curve fitted to the net heat output, exhibited a much better fit of the data ($R^2 = 0.98$) than before subtraction ($R^2 = 0.77$). This analysis demonstrates that any remaining energy relating to metabolic heat output in rested muscle has effectively disappeared by 12 h, with the time to halving of heat output estimated as 2.3 h. From the curve we estimated a starting metabolic output (intercept) in rested muscle of 417 $\mu W\,g^{-1}$. We presume this to be an anaerobic metabolic rate in the tissue at the time of death, although it could be elevated by tissue damage associated with the preparation of the biopsies. For example, tissue wounding of plant tissue increases metabolic heat output [43].

Similar to our findings, an exponential decline in metabolic rate has been reported in adult, infantile and neonatal rat myocardial tissue over a 3.5 h period [44]. The metabolic rates were significantly higher in neonatal and infantile rat hearts, declining exponentially from around 4.5 and 2.5 $mW\,g^{-1}$ (dry weight) to around 1 $mW\,g^{-1}$ and 400 $\mu W\,g^{-1}$ respectively over 90 min. The authors term these "dying curves". Of interest is that these authors report a period before the exponential decline of about 10 min where metabolic rate drops more slowly, indicating that tissue homeostasis may have been partially sustained. There is no evidence of this in our data, although we could not measure metabolic heat output reliably over the first 30 min. Another study that has identified an exponential decline in anaerobic heat output [45] makes for an interesting comparison. These authors report a non-sustainable heat output by human legs during cycling of >800 W that decreases exponentially over a 5 min period. This trend is attributed to creatine phosphate and glycogen availability in the "effectively hypoxic/anoxic skeletal leg muscles". These data corroborate our findings and are supportive of the idea that reduced ATP supply from anaerobic glycolysis and ADP phosphorylation, via the creatine kinase pathway, contribute to an exponential decline in metabolic rate (heat output) in muscle.

Interestingly, the initial estimated resting heat output for our salmon white muscle is in the same range as values recorded for whole fish. In goldfish held at 20 °C in a flow-through calorimeter the normoxic heat output was 400 $\mu W\,g^{-1}$, falling to 250 $\mu W\,g^{-1}$ during exposure to 3% of the normoxic PO_2 [46]. Tilapia (*Tilapia mossambica*) at the same temperature had a heat output of 448 $\mu W\,g^{-1}$ in light conditions and 317 $\mu W\,g^{-1}$ in the dark [47]. Similar values are also reported in experiments using a constantly perfused myocardial calorimetry apparatus measuring aerobic heat output in hibernator and non-hibernator mammalian myocardial tissue slices [48]. These values ranged between about 500 $\mu W\,g^{-1}$ and 2 $mW\,g^{-1}$, and were temperature (20 and 37 °C) and hibernation-state dependent. Interestingly, their lowest values are close to our predicted anaerobic heat output of 417 $\mu W\,g^{-1}$ at time zero. The similarity in the values between our isolated muscle and reported whole-animal heat output values from both endo- and ectothermic vertebrate animals may relate to fact that a large proportion of the somatic mass is attributable to skeletal muscle (ca. 40–50%). Given this large contribution to the body mass, it is not surprising that our mass specific value for isolated muscle is similar to that produced by whole animals at rest.

Contrasting with the rapid rundown of metabolic rate in salmon white muscle, brain tissue slices from the anoxia-tolerant crucian carp showed only a one-third decrease in heat production from oxygenated values (from 600 to 400 $\mu W\,g^{-}1$) over an 18 h period of anoxia, which subsequently increased to resting values upon reoxygenation [49]. The extraordinary hypoxia tolerance and ability to ferment pyruvate to ethanol in this animal [33,50] may explain this phenomenal observation. At the lower end of the spectrum, maximum heat output that the working, perfused hagfish heart could maintain solely through anaerobic metabolism was estimated at 280 $\mu W\,g^{-1}$, and in this case the heart was able to export lactate as it was produced [51]. At the other extreme, a report of heat outputs of between 21 and 24 $mW\,g^{-1}$ in sea scorpion (*Myxocephalus scorpius*) white muscle during "C-shaped fast-starts" greatly exceeds our values [52]. These measurements are in close agreement with Johnson and Johnston [53], although Franklin and Johnston [54] reported 3-fold lower maximal heat output values in the Antarctic fish *Notothenia coriceps*. These relatively high values from teleost fish are sustainable only for extremely brief periods, and their relationship to resting metabolic rate is not clear.

Glycogen fell over the first 4 h concurrent with but not stoichiometric with the rise in lactate concentration (Fig. 2C). The source of the additional lactate in the exhausted animals is not clear as there were only around 5 $\mu mol\,g^{-1}$ glucose glucosyl units and 2 $\mu mol\,g^{-1}$ glycogen glucosyl units present in the tissue immediately post-mortem, and yet lactate concentration increased by close to 25 $\mu mol\,g^{-1}$, which would require 12.5 $\mu mol\,g^{-1}$ glucose. The rise in the rested group is also 20% higher than predicted if glucose was its only source. This discrepancy may reflect substrate recruitment from other, unknown sources since glucose concentrations do not fall to zero at 4 h, remaining between 2 and 4 $\mu mol\,g^{-1}$. Our high lactate values, which were as high as 70 $\mu mol\,g^{-1}$ in the exhausted treatment, may have exceeded the rested values due to lipid and/or protein oxidation, which generates glyceraldehyde and pyruvate respectively, before death. These metabolites could later have been converted to lactate. High tissue lactate values (up to 80 $\mu mol\,g^{-1}$) in post-mortem muscle have also been reported in white muscle of yellow-eyed mullet (*Aldrichetta forsteri*) and New Zealand snapper (*Pagrus auratus*) in a hyperoxic hyperbaric atmosphere [3] and in thawed tissue following frozen storage in Chinook salmon [55] which were all greater than predicted by carbohydrate stores. Investigation of the source of the additional lactate could form the basis of future work.

AMP increased greatly over the first 5 h post-mortem in rested tissue, the exhausted tissue producing less (Fig. 4C). This event could represent a significant means of managing hypoxia in muscle. Recently, Jibb and Richards [56] demonstrated an AMP concentration-dependent activation of AMP-activated protein kinase (AMPK) in hypoxic goldfish. AMPK is known to have a multitude of effects in white muscle, many of which can enhance anaerobic ATP generation and may also play a role in metabolic rate suppression by decreasing protein synthesis [56]. If these same processes are activated in salmon muscle it is possible that some of the decline in metabolic rate, and by inference ATP supply, may be attributable to AMPK activity, while the enzyme remained viable.

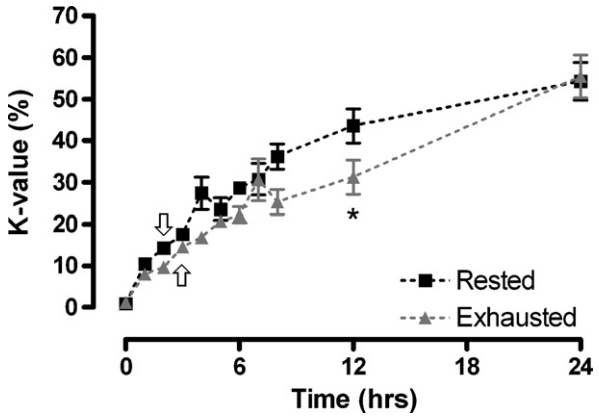

Fig. 7. *K*-values from rested (black squares) and exhausted (grey triangles) anoxic salmon white muscle at 10 °C over a 24 h period. $^{*}P < 0.05$ (two-way repeated measures ANOVA with Bonferroni post hoc test). White arrows indicate the first significant change in *K*-value of the dataset. Data are mean ± SEM. $n = 4$.

Inosine, hypoxanthine and uric acid concentrations showed a progressive rise over 24 h, while IMP concentrations peaked over the first 2 h (Fig. 5) and then gradually declined in both groups. Hypoxanthine was significantly lower after 24 h and IMP dropped significantly quicker in the rested group, but the general trend is similar in both groups and must therefore reflect the time of death more than the pre-harvest treatment. Consistent with these trends, Aubourg et al. [25] reported increases in the concentrations of inosine and hypoxanthine and a sharp drop in IMP over the first 24 h of storage at 2 °C in coho salmon (*Oncorhynchus kisutch*) white muscle fillets. The relatively stable total nucleotide pool (Fig. 6A) in both groups over time gives us confidence in our analytical methods.

The *K*-value represents the ratio of the sum of hypoxanthine and inosine to a pool of relevant ATP related compounds, and is frequently used as an indicator of freshness in fish muscle [25]. The *K*-value in both groups in the current study rises from 0 to 55% over 24 h, the exhausted group being significantly lower at 12 h (Fig. 7). The *K*-value in our study was greatly influenced by the inosine concentration in the tissue; the inosine values being approximately 10-fold higher than those of hypoxanthine. The end *K*-value of 55% after only 24 h is markedly greater than the 30% reported in coho salmon after 24 h [25], which suggests a greater rate of autolysis. This may reflect the relatively small size of the tissue biopsies used in the current study (1 cm^3).

Consistent with this idea is recent work from our laboratory [28], which indicates that whole fillets retain potential energy in the form of glycogen, creatine phosphate and ATP and maintain pH longer than the small muscle biopsies used in the current study, despite this preparation being maintained at 5 °C warmer. The slower depletion of high energy metabolites and change in pH illustrate a potentially important finding: that processing of muscle tissue (i.e. filleting, portioning) should be left to the latest possible time to maintain maximal metabolite stores.

Temperature differences may also partially explain the relatively rapid rate of *K*-value increase in the current study. The storage temperature in our study was 8 °C warmer than coho white muscle in the [25] study. This would have accelerated biochemical reactions by mass action effects. Assuming a conservative Q_{10} of 2, the estimated *K*-value of coho at 10 °C would be 48%, close to our value (55%). Had we maintained our preparation at refrigeration temperature, we would have expected a much slower rate of metabolism and associated metabolite depletion. Active behavioural selection of cold temperature is used as an adaptive strategy for metabolic rate suppression in ectotherms, e.g. aestivating frogs [57]. Furthermore, a refrigeration temperature of about 4–5 °C would be approximately half the acclimation temperature, which is reported to be optimal for post-mortem white muscle storage [58,59]. Our data further highlights the importance of rapidly chilling tissues to slow metabolite depletion.

Further to the positive effects of rested harvesting in maintaining metabolic rate and energy charge in muscle (current study), this practice has been shown to reduce cortisol secretion and lactate accumulation in "stressed" channel catfish (*Ictalurus punctatus*) (confined, low oxygen conditions) [21], retard spoilage in Chinook salmon [2] and improve meat quality indicators in Atlantic salmon (*Salmo salar*) [14]. Thus the additive effects of rested harvesting have a significant impact on the physiology, quality, freshness and shelf-life of harvested products.

5. Conclusions

We have studied anaerobic metabolism and energetics in the white muscle of a commercially harvested teleost (Chinook salmon) subjected to different harvest regimens. We measured anaerobic metabolic rate using calorimetry and assayed key metabolites associated with energy supply. The effect of harvest regimen was pronounced; the anaesthetised and rested animals having a markedly elevated metabolic rate and concentration of metabolites above the exhausted group for a period post-mortem. The exponential decline in anaerobic metabolic rate from the rested group was highly correlated with exponential declines in the concentrations of ATP, creatine phosphate and glycogen which were the most likely source of the observed differences in heat output between treatments. These data corroborate earlier reports that harvesting associated with modest pre-mortem activity can retain energy stores and extend tissue viability in muscle.

Acknowledgements

LGF was supported by a Plant and Food Research scholarship. Thanks to Isaac Salmon Farm for animals and facilities. Thanks to Drs. Thomas Hughes of Chemical and Process Engineering and Steven Gieseg of the Free Radical Research Laboratory for valuable advice on analytical procedures.

References

[1] R.W. Zabel, C.J. Harvey, S.L. Katz, T.P. Good, P.S. Levin, Am. Sci. 92 (2003) 150–158.
[2] G.C. Fletcher, V.K. Corrigan, G. Summers, M.J. Leonard, A.R. Jerrett, S.E. Black, J. Food Sci. 68 (2003) 2810–2816.
[3] S.E. Black, A.R. Jerrett, M.E. Forster, J. Food Sci. 69 (2004) 297–302.
[4] B.G. Bosworth, B.C. Small, D. Gregory, J. Kim, S.E. Black, A.R. Jerrett, Aquaculture 262 (2007) 302–318.
[5] I.A. Johnston, P.S. Ward, J. Fish Biol. 7 (1975) 451–458.
[6] Q. Bone, in: W.S. In, D.J. Hoar, Randall (Eds.), Locomotor Muscle, Fish Physiology, vol. 7, Academic Press, New York, 1978, pp. 361–424.
[7] S.J. Peake, A.P. Farrell, J. Exp. Biol. 207 (2004) 1563–1575.
[8] C.L. Milligan, Comp. Biochem. Physiol. 113A (1996) 51–60.
[9] P.M. Schulte, C.D. Moyes, P.W. Hochachka, J. Exp. Biol. 166 (1992) 181–195.
[10] Y. Wang, G.J. Heigenhauser, C.M. Wood, J. Exp. Biol. 195 (1994) 227–258.
[11] A.R. Jerrett, J. Stevens, A.J. Holland, J. Food Sci. 61 (1996) 527–532.
[12] T. Sigholt, U. Erikson, T. Rustad, S. Johansen, T.S. Nordtvedt, A. Seland, J. Food Sci. 62 (1997) 898–905.
[13] A.R. Jerrett, A.J. Holland, J. Food Sci. 63 (1998) 48–52.
[14] A. Kiessling, M. Espe, K. Ruohonen, T. Mørkøre, Aquaculture 236 (2004) 645–657.
[15] B. Roth, E. Slinde, J. Arildsen, Aquaculture 257 (2006) 504–510.
[16] M. Bagni, C. Civitareale, A. Priori, A. Ballerini, M. Finoia, G. Brambilla, G. Marino, Aquaculture 263 (2007) 52–60.
[17] L. Ribas, R. Flos, L. Reig, S. MacKenzie, B.A. Barton, L. Tort, Aquaculture 269 (2007) 250–258.
[18] R.J. Wilkinson, N. Paton, M.J.R. Porter, Aquaculture 282 (2008) 26–32.
[19] G.R. Stehly, W.H. Gingerich, Aquacult Res. 30 (1999) 365–372.
[20] M. Iversen, B. Finstad, R.S. McKinley, R.A. Eliassen, Aquaculture 221 (2003) 549–566.
[21] B.C. Small, Aquaculture 283 (2004) 469–481.
[22] J.C. Ingvast-Larsson, V.C. Axén, A.K. Kiessling, Am. J. Vet. Res. 64 (2003) 690–693.
[23] R.J. Connett, Am. J. Physiol. 254 (1988) R949–R959.

[24] P.G. Arthur, M.C. Hogan, D.E. Bebout, P.D. Wagner, P.W. Hochachka, J. Appl. Physiol. 73 (1992) 737–742.
[25] S.P. Aubourg, V. Quitral, M.A. Larrain, A. Rodriguez, J. Gomez, I. Maier, J. Vinagre, Food Chem. 104 (2007) 369–375.
[26] R.C. Summerfelt, L.S. Smith, Anesthesia, surgery, and related techniques, in: C.B. Schreck, P.B. Moyle (Eds.), Methods for Fish Biology, American Fisheries Society, Bethesda, 1990, pp. 213–272.
[27] D. Keppler, K. Decker, Glycogen: determination with amyloglucosidase, in: H.V. Bergmeyer (Ed.), Methods of Enzymatic Analysis, Academic Press, New York, 1974, pp. 1127–1131.
[28] N.P.L. Tuckey, Technologies for tissue preservation: the role of endogenous antioxidants in preserving tissue function in Chinook salmon, *Oncorhynchus tshawytscha*, Ph.D. Thesis, University of Canterbury, Christchurch, 2008, pp. 81–106.
[29] P.W. Hochachka, G.B. McClelland, J. Exp. Biol. 200 (1997) 381–386.
[30] M.C. Hogan, P.G. Arthur, D.E. Bebout, P.W. Hochachka, P.D. Wagner, J. Appl. Physiol. 73 (1992) 728–736.
[31] P.W. Hochachka, PNAS 96 (1999) 12233–12239.
[32] P.W. Hochachka, J. Exp. Biol. 206 (2003) 2001–2009.
[33] I.A. Johnston, Comp. Biochem. Physiol. 51B (1975) 235–241.
[34] C.L. Milligan, C.M. Wood, Physiol. Zool. 60 (1987) 37–53.
[35] C.L. Milligan, D.G. McDonald, J. Exp. Biol. 135 (1988) 119–131.
[36] A. Pagnotta, C.L. Milligan, J. Exp. Biol. 161 (1991) 489–508.
[37] P.M. Thomas, N.W. Pankhurst, H.A. Bremner, J. Fish Biol. 54 (1999) 1177–1196.
[38] G. van den Thillart, A. Waarde, H.J. Muller, C. Erkelens, A.D.F. Addink, J. Lugtenburg, Am. J. Physiol. 256 (1989) R922–R929.
[39] J.G. Richards, A.J. Mercado, C.A. Clayton, G.J.F. Heigenhauser, C.M. Wood, J. Exp. Biol. 205 (2002) 2067–2077.
[40] J.D. Kieffer, D. Alsop, C.M. Wood, J. Exp. Biol. 201 (1998) 3123–3133.
[41] J.G. Richards, G.J.F. Heigenhauser, C.M. Wood, Am. J. Physiol. 282 (2002) R89–R99.
[42] N.V. Prabhu, K.A. Sharp, Ann. Rev. Phys. Chem. 56 (2005) 521–548.
[43] L. Wadsö, F. Gomez, I. Sjoholm, P. Rocculi, Thermochim. Acta 422 (2004) 89–93.
[44] C. Mühlfeld, D. Singer, N. Engelhart, J. Richter, A. Schmeiedl, Comp. Biochem. Physiol. 141A (2005) 310–318.
[45] K.E. Conley, W.F. Kemper, G.J. Crowther, J. Exp. Biol. 204 (2001) 3189–3194.
[46] V.J.T. van Ginneken, P. Snelderwaard, R. van den Linden, N. van den Reijden, G.E.E.J.M. van den Thillart, K. Kramer, Thermochim. Acta 414 (2004) 1–10.
[47] V.J.T. van Ginneken, A.D.F. Addink, G.E.E.J.M. van den Thillart, F. Körner, L. Noldus, M. Buma, Thermochim. Acta 291 (1997) 1–13.
[48] J. Ikomi-Kumm, M. Monti, A. Hanson, B.W. Johansson, Cryobiology 31 (1994) 133–143.
[49] D. Johansson, G.E. Nilsson, E. Tornblom, J. Exp. Biol. 198 (1995) 853–859.
[50] P.W. Hochachka, J. Exp. Biol. 115 (1985) 149–164.
[51] M.E. Forster, J. Exp. Biol. 156 (1991) 583–590.
[52] T.A. Beddow, L.J.V. Leuween, I.A. Johnston, J. Exp. Biol. 198 (1995) 203–208.
[53] T.P. Johnson, I.A. Johnston, J. Exp. Biol. 157 (1991) 409–423.
[54] C.E. Franklin, I.A. Johnston, J. Exp. Biol. 200 (1997) 703–712.
[55] D.G. Cook, A.J. Holland, A.R. Jerrett, M.E. Forster, J. Food Sci. 74 (2009) 543–548.
[56] L.A. Jibb, L.A.J.G. Richards, J. Exp. Biol. 211 (2008) 3111–3122.
[57] R.G. Boutilier, Resp. Physiol. 128 (2001) 365–377.
[58] A.R. Jerrett, R.A. Law, A.J. Holland, S.E. Cleaver, S.C. Ford, J. Food Sci. 65 (2000) 750–755.
[59] A.R. Jerrett, R.A. Law, A.J. Holland, S.E. Black, J. Food Sci. 67 (2002) 2843–2850.